5-2010

Biophysical Investigation of the Cataract Associated Mutant, E107A of Human Gamma-D Crystalline And Constructing a Fluorescent System for Manipulating PIP2 Concentration in the Plasma Membrane of Xenopus Oocytes.

Julita Patrosz
University at Albany, State University of New York

Biophysical Investigation of the Cataract Associated Mutant, E107A of Human Gamma-D Crystalline

And

Constructing a Fluorescent System for Manipulating PIP_2 Concentration in the Plasma Membrane of Xenopus Oocytes.

An honors thesis presented to the
Department of Biological Sciences,
University at Albany, State University
Of New York in partial fulfillment
of the Honors Program Requirements.

Julita Patrosz
2010

Department of Biological Sciences
University at Albany

This Honors Thesis has been read and approved
by the undersigned and is hereby recommended for acceptance.

Thesis Committee:

Research Advisor: _____

Signature: _____Date:_____

Research Advisor: _____

Signature: _____Date:_____

Member: _____

Signature: _____Date:_____

ACTION: Accepted ☐ Not Accepted ☐

_____ _____
Robert Osuna Date

Departmental Honors Program Director

ABSTRACT:

Chapter 1: Biophysical investigation of the cataract associated mutant, E107A of human gamma-D crystallin.

Several human genetic cataracts are associated with mutations in a single amino acid residue of the protein known as γD crystallin. Recently, the Glu107Ala (or E107A) mutation has been included in this list, and it has been associated with a nuclear congenital cataract. We have made recombinant human γD crystallin and its E107A mutant and conducted preliminary comparisons of its structure and biophysical properties with that of the wild-type protein. In this process we made use of several techniques – Circular Dichroism (CD), Iso-electric focusing (IEF) gels, Dynamic Light Scattering (DLS), and Nuclear Magnetic Resonance (NMR). Results highlight small structural changes while the overall protein structure remains folded and intact.

Chapter 2: Constructing a fluorescent system for manipulating PIP_2 concentration in the plasma membrane of Xenopus Oocytes.

Potassium channels play a key role in electric activity of excitable cells. Dysfunction of these ion channels may result in neuronal, cardiac, and muscular disorders. Several subfamilies of potassium channels are regulated via G-protein coupled receptor signaling pathway and the signaling molecule PIP_2 may affect potassium channel activity. To understand how PIP_2 regulates potassium channels, we are going to construct a unique fluorescent system to manipulate the PIP_2 levels in the plasma membrane of Xenopus oocytes, an ideal heterologous expression system for studying function of ion channels. We plan to heterologously express

membrane-attached FRB-CFP fusion protein and cytoplamic RFP-FKBP12-phosphoinositide 5-phosphatase fusion protein in Xenopus oocytes. Application of rapamycin will result in heterodimerization of a FKBP12 protein with FRB protein. This process will increase the concentration of phosphoinositide 5-phosphatase and lower the concentration of PIP_2 in the membrane of Xenopus oocytes. Accordingly the fluorescent signals will change during this process. With site-directed mutagenesis and sub-cloning strategies, we successfully made a construct that expresses RFP-FKBP12 fusion protein in Xenopus oocytes. This construct will be used as a negative control in this system.

Table of Contents

Chapter 1

Biophysical investigation of the cataract associated mutant, E107A of human gamma-D crystallin

INTRODUCTION:

Proteins are macromolecules that have diverse functions in the human body. They can be found virtually in every cell and are of many types: enzymes, antibodies, contractile proteins, hormonal proteins, and many more types.

The most abundant proteins found in the vertebrate eye lens belong to a group called crystallins, of which there are three major subgroups α, β, and γ, based on their decreasing molecular weights [1-3]. Those proteins are responsible for the refractive properties of the lens. α, β, and γ crystallins are encoded by CRA-, CRB-, and CRG- genes respectively [4]. Only the α-Crystallins were found to act as molecular chaperones and protect a lens against stress [4]. Those functions may be altered by mutations in CRAA and CRAB genes many of which are found to be associated with disorders such as cataract, desmin-related myopathy or dilated cardiomypathy [4].The β and γ crystallins were found to have mainly refractive properties [5]. Multiple single point mutations in one member of the γ-crystallin family, Human Gamma D crystallin, are linked to a number of well known cataract phenotypes. The CRGD gene is one of the most abundantly expressed γ –crystallin genes in the human lens [6-8].

Cataract belongs to a class of diseases commonly referred to as protein-misfolding disorders; however the disease associated mutation may or may not lead to conformational change [9-11]. Instead the protein undergoes a significant loss of solubility leading to the

formation of several insoluble phases that can be amorphous, crystalline, or gel-like [12] which lead to increased light scattering and opacity.

The P23T mutant in particular has been associated with coralliform, cerulean, and fasciculiform cataract phenotypes [13-15], whereas the E107A mutant has been associated with nuclear congenital cataract [16]. Both of these mutations are characterized as single point mutations of Human Gamma D (HGD) protein, and were found to be associated with formation of cataract in the human eye. In our laboratory we have focused on the latter mutation, which was observed specifically in nuclear congenital cataract. This disorder is characterized by opacity in the center portion of the eye lens and can be detected sometime before the first year after birth [16]. The E107A mutation involves a substitution of a negatively charged glutamic acid residue with a neutral alanine at position 107 along the amino acid sequence. This causes not only a change in the charge of the protein, but also a change in the size of the residue at this position, since alanine has a smaller side chain than glutamic acid.

As first step towards understanding the mechanism of how the E107A mutation leads to opacity, we proceeded to compare the solution structures and biophysical characteristics of the recombinant E107A mutant with wild-type HGD. We collected NMR, DLS and CD data for HGD and E107A and examined if there was a change in the pI of the native protein due to the mutation, using isoelectric focusing gels.

METHODS AND MATERIALS:

Expression and Isolation of the Protein:

In order to overexpress the protein (HGD and E107A mutant) the E. coli cultures, containing DNA encoding the protein, were grown in LB broth at 37˚C until the absorbance at 600 nm reached 0.6 (until induction). Isopropyl 1-thiol-D-galactopyranoside (IPTG) was added to induce expression of gamma crystallins and the cultures were grown in a M9 minimal medium containing ampicillin, containing 1 g/L [U–^{15}N]NH_4Cl and 2 g/L D-glucose (for [U-,^{15}N]-labeled protein). The growth was terminated when the absorbance at 600nm reached 1. Centrifugation was used to pellet the cells which then were resuspended in the NMR buffer (10 mM KPO_4 (pH 7.0), 100 mM NaCl, 0.02% NaN_3, 90% H_2O and 10% D_2O) containing complete protease inhibitor (1tablet/30mL, from Roche Molecular Biochemicals), followed by lysis initiated using lysozyme (250µg/mL, from chick egg white). Next, seven cycles of a freeze-thaw procedure were carried out in which the cell suspension was frozen in liquid nitrogen followed by thawing in water bath set to approximately 30˚C. Sonication procedure was then used for one minute at the highest power setting. DNase (1 mg/mL, Turbo DNAse from Ambion) was added to the resulting suspension which was then centrifuged at 48,400 x g for 15 minutes. Magnesium (8 mM) was added to the supernatant followed by one hour incubation and addition of DTT (10 mM). The final pH was brought to 4.5 with acetic acid. Concentration of the purified protein was determined using an extinction coefficient of 41.4 mM^{-1}•cm^{-1} at 280nm wavelength [17].

Nuclear Magnetic Resonance Spectroscopy:

The NMR spectroscopy data was collected by Mr. Jian Chao Zhang in collaboration with Prof. Alexander Shekhtman.

Data was collected at 25˚C in a Bruker Avance spectrometer, operating at 500 MHz ^{1}H frequency. In order to perform backbone chemical shift assignment standard double and triple resonance NMR experiments, 2D $^{1}H–^{15}N$ HSQC and 3D CBCA (CO)NH, HNCACO, HNCO, and HNCACB, were used [18]. TOPSPIN 2.1 (Bruker, Inc.) software was used to process all of the spectra and CARA software was used to perform the chemical shift assignments [19].

Circular Dichroism Spectroscopy:

The CD spectra were obtained by Dr. Ajay Pande.

CD spectra were obtained using a Jasco (Easton, MD) model J-810. Protein solutions were in 0.1M sodium phosphate buffer, pH 7. Concentration of 0.41mg/mL and 1.23mg/mL was used for E107A mutant and HGD samples respectively.

Quasielastic Light Scattering:

A Wyatt Dynapro MS/X dynamic scattering system with Peltier temperature control was used to measure the hydrodynamic radii and the size distribution of the particles in the protein

samples. Protein concentrations ranging from 1.25 mg/mL to 5.00 mg/mL were used in 0.1M sodium phosphate buffer, pH 7.

Isoelectric Focusing Gel Electrophoresis:

IEF gel electrophoresis was performed using the IEF Minicell from Bio-Rad. 5% acrylamide gel (5% acrylamide, 5% glycerol, 2% ampholyte, pH 3-10) was prepared. Gel solution was then degassed for 5 minutes followed by the addition of 0.2% TEMED, 0.03% APS, and 0.03% riboflavin 5'-monophosphate (FMN). The gel was left to solidify for about 45 minutes under an open fluorescent light. The gel was placed in the Minicell and current was applied using the PowerPac Basic Power Supply from Bio-Rad, for approximately 45 minutes. Following completion of the run, the gel was stained for one hour with shaking in IEF staining solution (27% Ethanol, 10% Acetic Acid, 0.04% Coomassie Brilliant Blue, 0.5% $CuSO_4$, 0.05% Crocein Scarlet). The gel was de-stained by incubating in de-staining buffer-I for an hour with shaking (12% Ethanol, 7% Acetic Acid, 0.5% $CuSO_4$), followed by overnight incubation with shaking in IEF de-stain II (25% Ethanol, 7% Acetic Acid). Protein bands were visualized on a Chemi-Doc gel documentation system from Bio-Rad labs.

Modeling:

The high resolution, 3D x-ray crystal structure of HGD was displayed by importing the coordinates from the Protein Data Bank and using the Swiss-PDB Viewer (PDB structure 1hk0; resolution 1.25Å; ref. 20).

Results:

Comparison of Isoelectric Point:

Isoelectric focusing (IEF) gels revealed an increase in the isoelectric point due to the mutation (Figure 1.1).

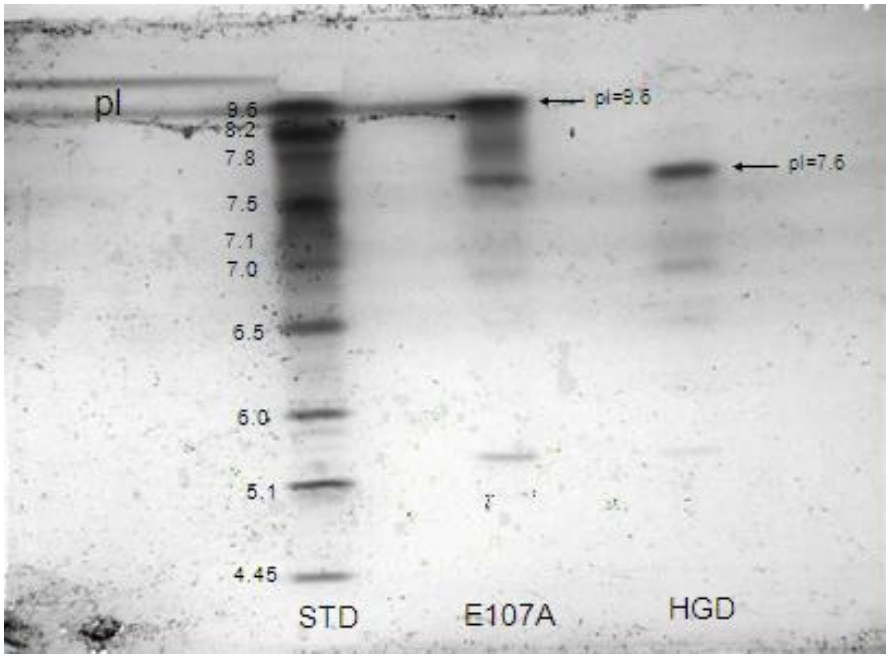

Fig. 1.1. **IEF gel for E107A mutant and native HGD protein.** The IEF standard (from Bio-Rad) can be seen on the left hand side (marked as STD). The middle band corresponds to the E107A mutant (2mg/mL). Native HGD protein (2mg/mL) was loaded on the right hand side of the gel. The mutant protein appears to have a pI value of 9.6 where as the wild type HGD protein appears to have pI of 7.6. The lower, less visible bands are most likely due to the post-translational modifications of the protein.

The most intense band on the IEF gel for E107A appeared at a pI of 9.6 for the mutant protein and around 7.6 for wild-type HGD. Lower, less intense bands can also be seen. These bands are typical for IEF gels and may be due to post-translational modifications of a protein such as deamidation. This observed difference in pI value was expected since the mutation leads to a change in the total charge of the protein.

Protein Structure Comparison:

In this project two spectroscopic windows were used in CD measurements, far and near UV, in order to gain an insight into the differences in secondary and tertiary structure of E107A and HGD (figures 1.2 and 1.3). The data obtained from the sample containing E107A mutant protein was overlaid with the wild-type HGD data. Far UV circular dichroism measurements reveal a strong positive peak at a wavelength of about 198 nm and a slight negative peak around 222 nm (figure 1.2).

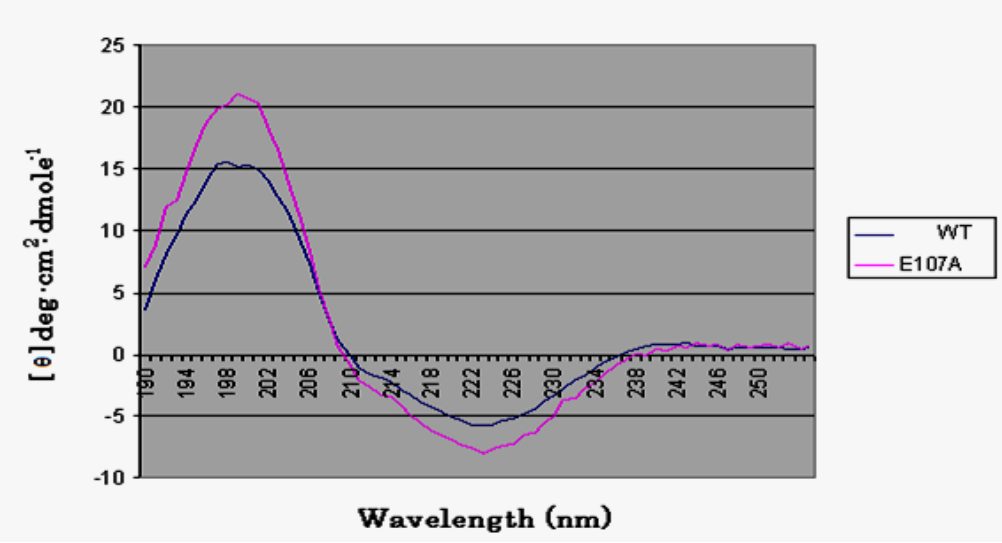

Figure 1.2. Far UV CD data for E107A (pink curve) and HGD (dark blue curve). The numerical data was converted into a graph which revealed a strong positive peak around 198 nm and a weaker, negative peak around 222 nm. This is indicative of the presence of β pleated sheets in both proteins. The two proteins seem to be composed mostly of those motifs. The data suggest that the single point mutation had no significant effect on the secondary structure of the protein.

This corresponds to a pattern consistent with a protein composed mostly of a β pleated sheet motif. The data shows that the structure of E107A remains predominantly β-pleated sheet and that the secondary structures of both proteins are nearly identical.

Data obtained in the near UV-CD region shows two strong, negative peaks, one around 290 nm and another around 300 nm (Figure 1.3). The close correspondence of the two curves again strongly suggests that the tertiary structures of the protein were not significantly altered by the single point mutation.

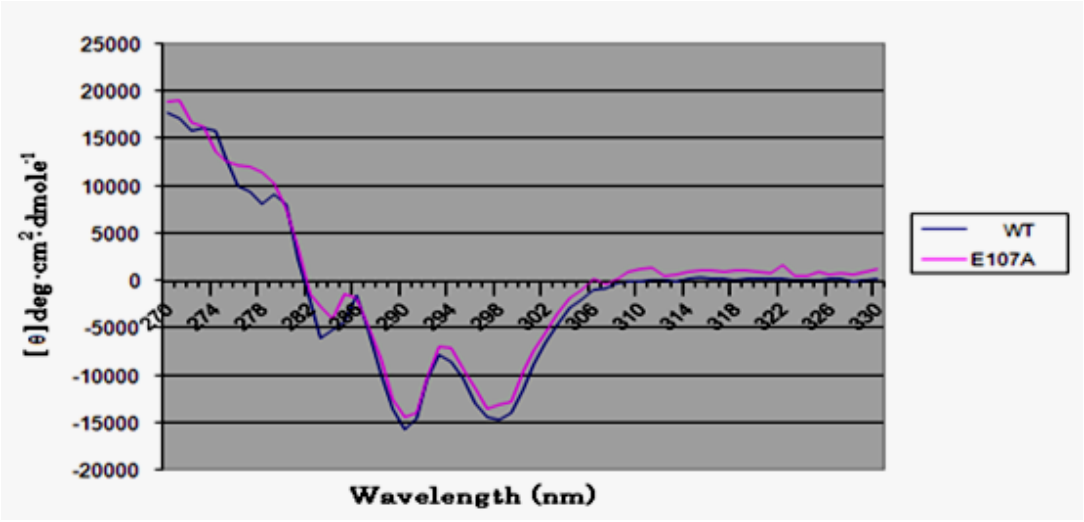

Figure 1.3. **Near UV CD data for E107A mutant (pink curve) and native HGD protein (dark blue curve).** The data obtained from near UV CD was used to create the above curves. In result two, relatively strong, negative peaks emerged in both curves, around a wavelength of 290nm and 300nm. Both pink and dark blue curve follow the same pattern and are nearly ideally superimposed on each other indicating that there was little or no change in the tertiary structure of the protein due to the single point mutation.

The NMR data was analyzed using Cara software. First about 90% of E107A mutant residues were assigned, and then the data corresponding to both native and mutant protein was overlaid on the HSQC spectrum (figure 1.4). Most of the peaks obtained from the NMR measurements of the two proteins appear in the same region on the HSQC spectrum.

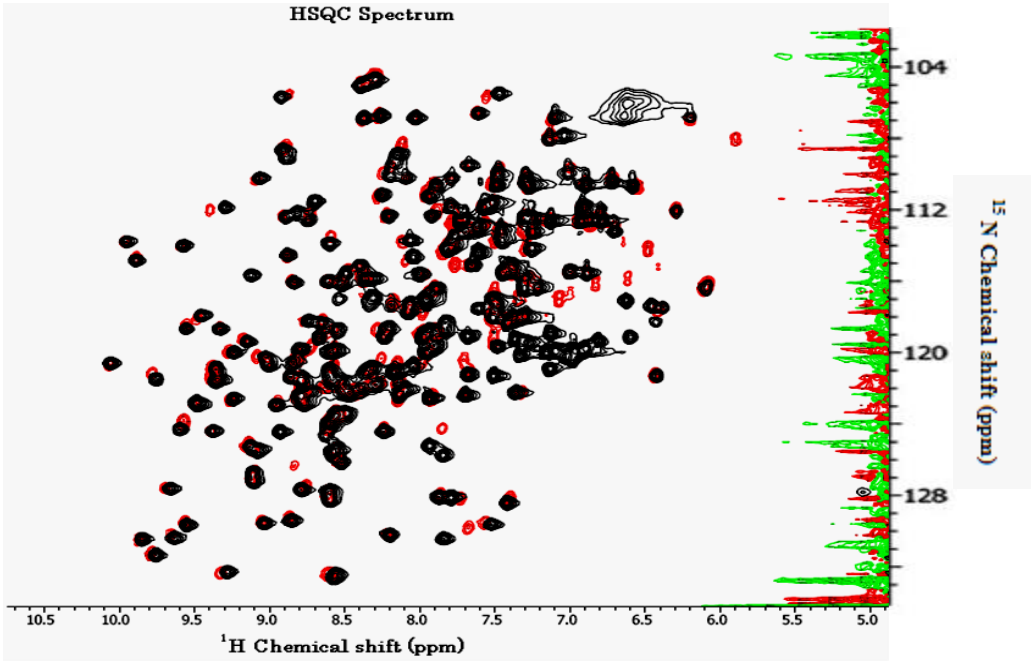

Figure 1.4. **NMR**, **HSQC spectrum for E107A (red) and HGD (black) protein.** The chemical shifts of the residues in both proteins produced a similar pattern. The data suggests that there is no significant difference between the two proteins and most of the peaks appear to be superimposable.

Like-Like, Protein-Protein Interactions Comparison:

Dynamic light scattering measurements were done on the mutant and wild-type proteins with concentrations ranging from 1.25mg/mL to 5.00 mg/mL. The data shows that there is no significant difference in like-like protein-protein interactions between the two protein species (figure 1.5, table 1.1). Hydrodynamic radius data collected for HGD were nearly identical to that collected for E107A. The largest difference in the size of the hydrodynamic radii of the two proteins was 0.06 nm. There was also little variation observed in the data corresponding to the percent polydispersity of E107A and HGD protein. The greatest difference in the obtained values was 1.6 %.

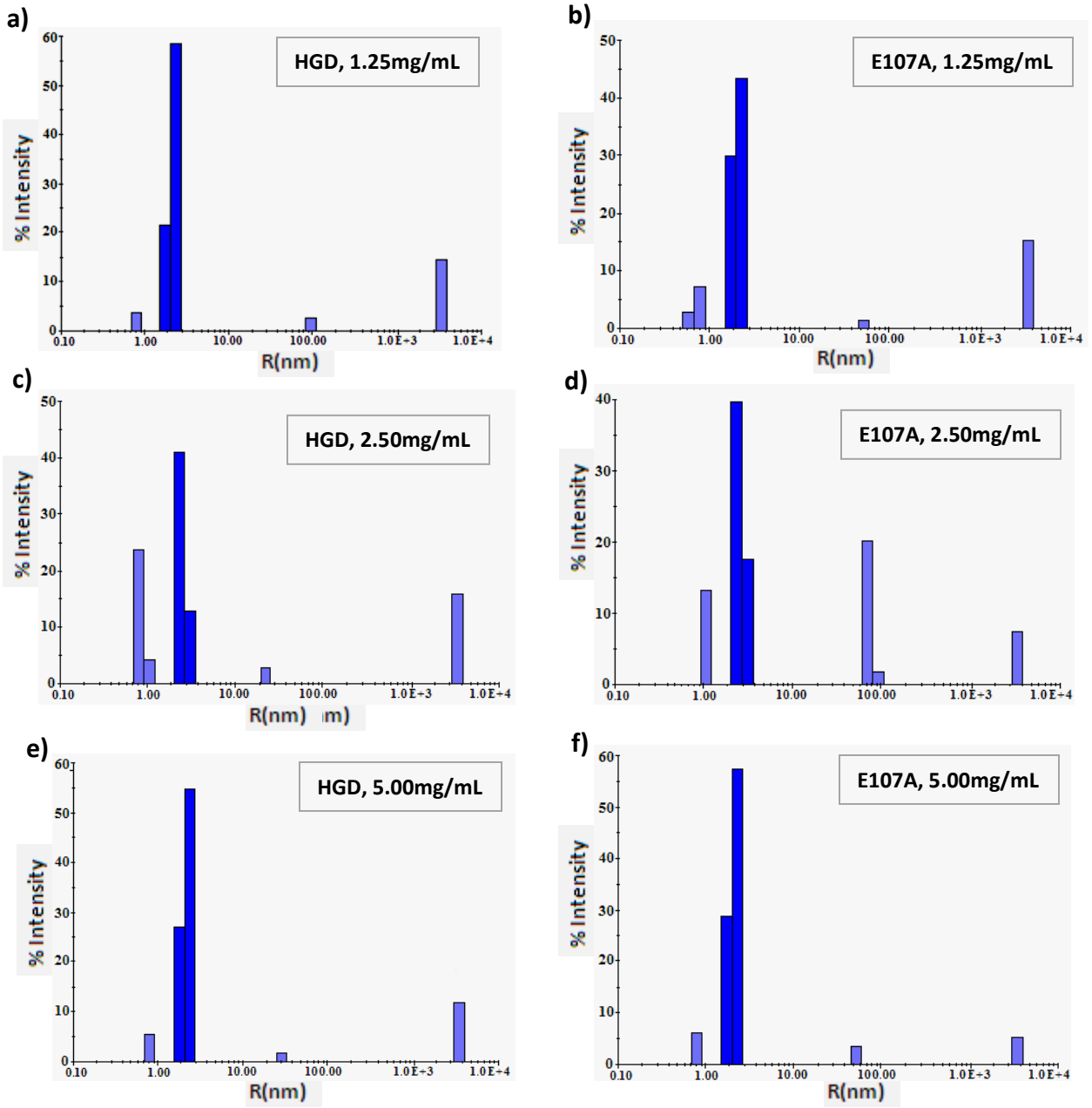

Fig. 1.5. **Dynamic Light Scattering Data.** Data collected using Dyna Pro DLS machine from Watt Technology were converted into histograms. This figure shows just a representative fraction of the DLS data that was collected in our laboratory. The light blue bars are due to impurities, such as dust, that were present in the sample. The dark blue bars represent the part of data that corresponds to the protein of interest. Each sample had either 1.25mg/mL (parts a and b), 2.5mg/mL(parts c and d), or 5.00mg/mL(parts e and f) concentration of the protein of interest. The data was collected for both E107A mutant (parts b,d, and f) and wild-type HGD (parts a,c, and e). This data was also tabulated (see table 1.1).

Table 1.1. DLS Data for 1.25mg/mL – 5.00mg/mL E107A mutant and 1.25mg/mL – 5.00mg/mL HGD protein.				
Concentration (mg/mL)	HGD		E107A	
	R(nm)	%Pd	R(mn)	%Pd
1.25	2.23	11.70	2.27	13.30
2.50	2.71	12.80	2.77	13.60
5.00	2.32	12.40	2.32	12.50

Percent polydispersity (%Pd) was quite low for both proteins. This indicates that all of the samples contained protein molecules in a monomeric state (%Pd ≤ 20%). This was expected for HGD but not for E107A.

Modeling:

The structure of E107A was modeled on the high resolution x-ray crystal structure of HGD which shows that Human Gamma D crystallin and its E107A mutant are composed of two domains (Figure1.6). The mutation site can be seen at the edge of the C-terminal domain. The acidic, additional carboxylate group of glutamic acid is shown in red.

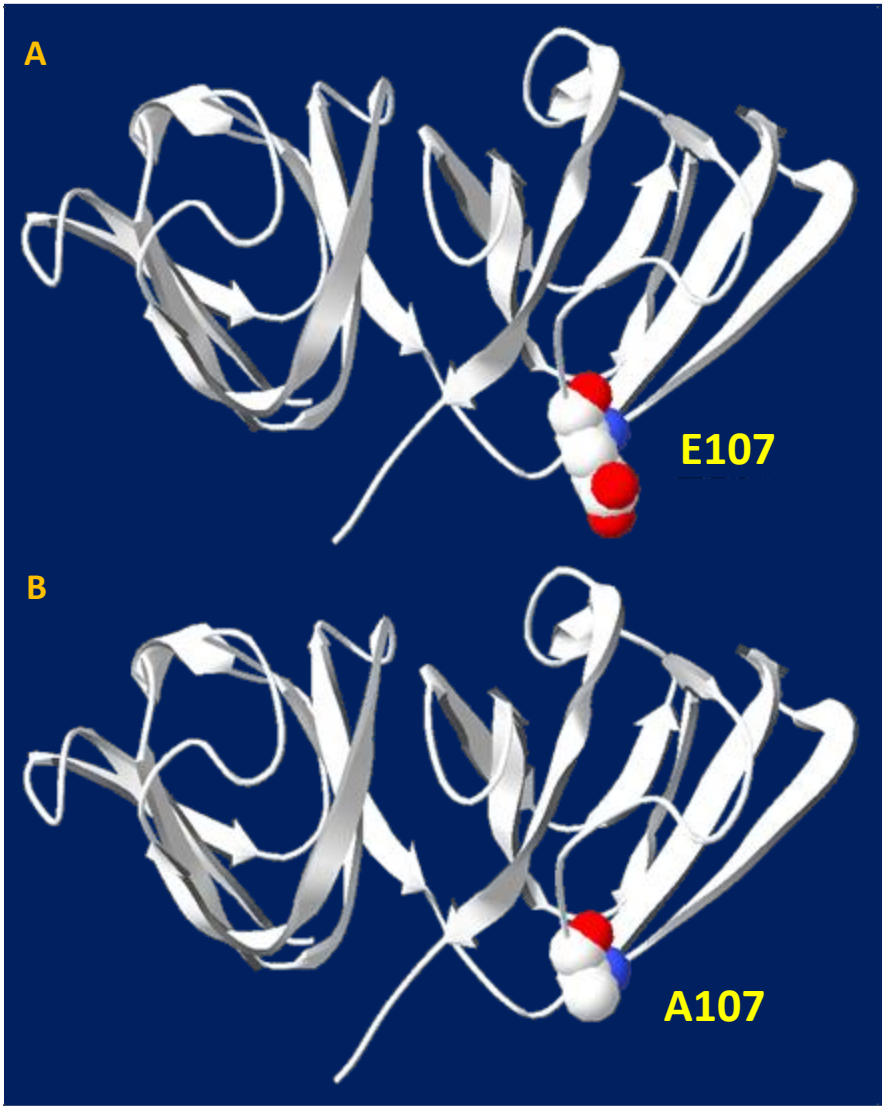

Fig. 1.6. A ribbon diagram of the x-ray structure of HGD [19] and the homology model of E107A. A) Human Gamma D protein with Glu107 involved in substitution shown as a space filling model. B) A model of E107A using PDB viewer software, showing A107 residue as a space filling model.

DISCUSSION:

We have shown that the isoelectric point of E107A mutant is higher than the isoelectric point of negatively charged HGD protein. Preliminary data show that the observed difference was about two pI points. One of the sources notes that the isoelectric point of gamma-D crystallins in mammals ranges from pH7.1 to pH 8.6 [4], which is consistent with our findings for

HGD of about 7.6. While we expected a higher pI value for E107A based on the nature of the amino acid substitution, the actual magnitude of 9.6 may not be accurate because the IEF standard used has a low resolution in the pI range of 7.8 to 9.6. This made it difficult to obtain a better estimate of the pI value for the E107A mutant.

Using Dynamic Light Scattering, we have also shown that there are no significant changes in like-like protein-protein interactions in E107A compared to HGD. Both proteins show a low percentage of polydispersity and are predominantly monomeric, which indicates that neither protein undergoes aggregation under our measurement conditions. The hydrodynamic radii of both proteins also appeared to be the same, and are about 2.43 nm. This finding shows that the shape of the molecule did not change due to the amino acid substitution. From this observation we can conclude that the size distribution properties of E107A mutant and native HGD protein are the same when the protein concentration ranges from 1.25mg/mL to 5.00mg/mL. There exists a small possibility that the results will differ if the measurements are taken for the proteins at their physical concentration, 300-400 mg/mL.

Similarly, based on our current results, the amino acid substitution does not seem to have an influence on the secondary or tertiary structure of the protein. This is shown in the results from circular dichroism and NMR measurements. High dispersion of the peaks in both ^{15}N and ^{1}H dimensions on HSQC spectrum (Figure 1.4) indicates that the protein structure (of both E107A mutant and native HGD) is well folded. This is confirmed by the far UV CD spectrum (Figure 1.2) which indicates that both protein species are composed mostly of β pleated sheet motifs and very little if any random coil regions. If the tertiary structure of the protein was in a

random coil state then the near UV CD spectra of the mutant would not resemble that of the wild-type. Since our data shows a clear near UV CD spectra for both E107A mutant and native HGD, we can conclude that both protein species are well folded. This is consistent with all of our results. The small differences in CD spectra of both proteins may be due to the loss of a hydrogen bond; this is a result of substitution of polar residue by non-polar residue. Difference in far-UV CD spectra around 200 nm wavelength is most likely due to a small reorganizations in the peptide backbone.

Our data suggest that the cataract-associated E107A mutation is very similar to wild-type HGD in its secondary and tertiary structure and like-like protein-protein interactions. Thus, the manner in which it leads to increased light scattering and opacity is still unclear. However, in this project we have only examined like-like protein-protein interactions. The question remains as to what will happen if we look at interactions between E107A and a crystallin species other than human gamma-D crystallin. Since the other major class of water soluble proteins in the lens is alpha-crystallin, it is reasonable to assume that there might be differences in the interaction between E107A and the alpha crystallin. Such an interaction may reveal how the E107A mutation leads to like-unlike protein aggregation, increased light scattering and opacity in the affected eye lens.

CONCLUSION:

In our project we have shown that there are no significant conformational changes observed in the cataract-associated E107A mutant compared to the wild-type HGD protein. We

have also shown that the secondary structure of both proteins is composed predominantly of β-sheet. This mutation is the first example in which the like-like protein-protein interactions in a cataract-associated mutant of human γD crystallin are indistinguishable from those of the wild-type, such that the mutant protein is as soluble as the wild-type, and no novel light scattering elements (e.g. crystals, fibers or gels) are formed. Thus, the question of how this mutation leads to increased light scattering and lens opacity remains to be addressed.

ACKNOWLEDGEMENTS:

-NMR data taken by Mr. Jian Chao Zhang in collaboration with Prof. Alexander Shekhtman.

-CD data taken by Dr. Ajay Pande.

This work was supported by an RO1 grant from the National Institutes of Health to Professor Jayanti Pande.

REFERENCES:

1. Mörner CT (1893) *Z Physiol Chem* 18:61-106.
2. Siezen JR, Fisch RM, Slingsby C, Benedek BG (1985) *Proc Natl Acad Sci* 82:1701-1705.
3. Vérétout F, Delaye M, Tardieu A (1989) J Mol Biol 205:713–728.
4. Graw J (2009) *Experimental Eye Research* 88:173-189.
5. Tomarev IS (1996) *Eur J Biochem* 235:449-465.
6. Aarts HJ, den Dunnen JT, Leunissen J, Lubsen NH, Schoenmakers JG (1988) *J Mol Evol* 27:163-172.
7. Hejtmancik JF (1998) *Am. J. Hum Genet* 62:520-525.
8. Santhiya ST, Shyam Manohar M, Rawlley D, Vijayalakshmi P, Namperualsamy P, Gopinath PM, Loster J, Graw J (2002) *J Med Genet* 39:352-358.
9. Kmoch S, Brynda J, Befekadu A, Bezouška K, Novák P, Rezácová P, Ondrová L, Filipec M, Sedlácek J, Elleder M (2000) *Hum Mol Genet* 9:1779-1786.
10. Pande A, Pande J, Asherie N, Lomakin A, Ogun O, King AJ, Lubsen HN, Walton D, Benedek BG (2000) *Proc Natl Acad Sci* 97:1993-1998.
11. Pande A, Pande J, Asherie N, Lomakin A, Ogun O, Kind J, Benedek BG (2001) *Proc Natl Acad Sci* 98:6116-6120.
12. Pande A, Annunziata O, Asherie N, Ogun O, Benedek BG, Pande J (2005) *Biochemistry* 44:2491-2500.
13. Pande A, Anunziata O, Asheric N, Ogun O, Benedek GB, Pande J (2005) *Biochemistry* 44:2491-2500.
14. Evans P, Wyatt K, Wistow GJ, Bateman OA, Wallace B, Slingsby C (2004) *J Mol Biol* 343:435-444.
15. Khan OA, Aldahmesh AM, Ghadhfan EF, Al-Mesfer S, Alkuraya SF (2009) *Mol Vis* 15:1407-1411.
16. Messina-Baas MO, Gonzalez-Huerta ML, Cuevas-Covarrubias AS (2006) *Mol Vis* 12:995-1000.
17. Andley UP, Mathur S, Griest TA, Petrash JM (1996) *J Biol Chem* 271:31973-31980.
18. Cavanagh J, Fairbrother JW, Palmer GA, Rance M, Skelton JN (2007) "Protein NMR Spectroscopy: Principles and Practice, second ed." Academic Press, Amsterdam, Boston, pp.533–678.
19. Masse EJ, Keller R (2005) *J. Magn. Reson.* 174:133–151.
20. Basak AK, Bateman O, Slingsby C, Pande A, Asherie N, Ogun O, Benedek G, Pande J (2003) *J Mol Biol* 328:1137-1147.

Chapter 2

Constructing a fluorescent system for manipulating PIP_2 concentration in the plasma membrane of Xenopus Oocytes.

INTRODUCTION:

Malfunction of potassium ion channels can cause disorders such as hypokalemic periodic paralysis (hypoPP) [1], congenital deafness [2], or long-QT syndrome, a type of cardiac arrhythmia [3]. These channelopathies can be prevented by altering the activity of ion channels, which induces a change in blood potassium concentration. One possible way to accomplish this could be through alteration of phosphatidylinositol 4,5-biphosphate(PIP_2) concentration in the cell membrane.

PIP_2 Concentration was found to influence the function of transporters and several ion channels such as [4] (KCNQ1/KCNE1), voltage-gated potassium channels [5], and cardiac sodium-calcium exchangers (NCX1) [6]. It is a molecule that serves as a signaling phospholipid of the plasma membrane and it constitutes a large portion of total phosphoinositide species in mammalian cells [7]. Fluctuations in PIP_2 concentration were shown to influence the activity of KCNQ and other ion channels. For example, Binding of PIP_2 activates KCNQ K^+ channels [8]. Similarly hydrolysis of PIP_2 by phospholipase C can cause depletion of PIP_2 in the cell membrane that leads to reduction in the activity of KCNQ K^+ ion channels. It was speculated that those changes in PIP_2 concentration could be caused by factors such as aging, affective states or simply stress [9].

In order to determine the extent to which PIP_2 concentration influences activity of ion channels one must be able to visualize this signaling molecule in a cell and alter its

concentration without disturbing cell's integrity. This task was accomplished in few laboratories by creating a system with two protein constructs. One construct consists of a fluorescent protein fused to the pleckstrin homology (PH) domain of human PLC 1 that specifically binds PIP_2 and another one consists of mRFP-FKBP12 fusion protein and an enzyme (for example phosphoinositide 5-phosphatase)[7, 10, 11]. Fluorescent protein domains, mRFP and FKBP12 domain, enable visualization of the changes in PIP_2 concentration, where as FRB and FKBP12 protein domains allow for the two protein constructs to heterodimerize in the presence of rapamycin. This leads to subsequent hydrolysis of PIP_2 by the enzyme present in the second protein construct.

Before heterodimerization, there should be two distinct colors seen under the fluorescent microscope due to CFP and FKBP12 domain (blue and red color respectively). Upon heterodimerization of the two protein constructs we expect an appearance of one uniform color instead of two. This way we should be able to determine a relative position of the two constructs in Xenopus oocytes.

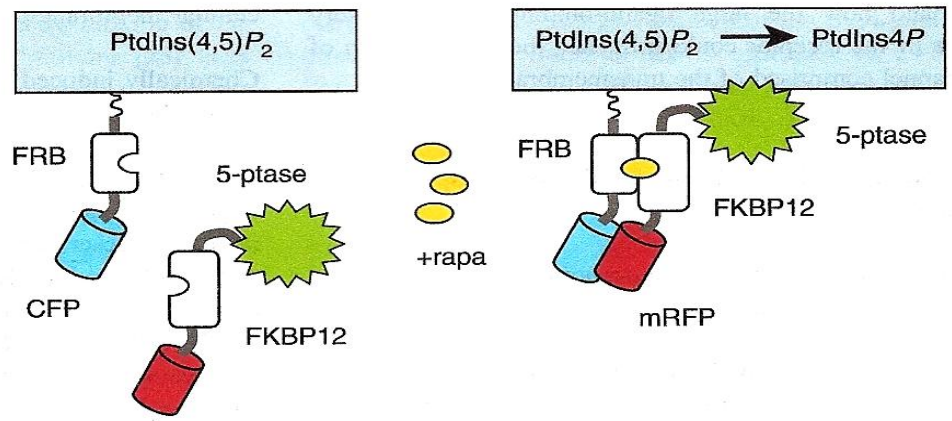

Figure 2.1. Protein constructs used in rapamycin induced targeting of 5-phosphatase to specific sites at the cell membrane. *This figure depicts the process in which FKBP12 protein domain heterodimerizes with a FRB protein domain, in a process that is a principle of drug-induced targeting. [11]*

All of those constructs were tested only in mammalian cells. We are planning to create similar constructs that will later on be used to test the effects of PIP_2 concentration on the activity of different potassium ion channels using Xenopus oocyte as a model organism. Unlike mammalian cells, Xenopus oocytes have their own source of nutrients, which causes no need for an external media to support cell growth. Other advantages of using Xenopus oocytes as a model organism rather than mammalian cells, include but are not limited to their large size, extremely high capacity for protein synthesis (200-400 ng protein per day per oocyte), and relative abundance [12]. There can be more electrochemical measurements done in one day using Xenopus oocyte than with a mammalian cell. Stage VI Xenopus oocyte is approximately 10^5 times larger than a nucleus of a mammalian, this will enable us to visualize the changes in the oocyte much easier than when using a mammalian cell [12]. More importantly, the available technology enables injection of the constructs without altering the integrity of the cell.

In this project we were able to successfully create a construct that will be used in expression of a mRFP-FKBP12 fusion protein in Xenopus oocytes. This will be used as a negative control in the system shown in figure 2.1.

METHODS AND MATERIALS

PCR:

PCR was used to introduce Hind III cut site into a mRFP-FKBP12 domain containing plasmid (pERFP). A 50µL PCR reaction was prepared using approximately 200ng of pERFP plasmid, 0.5µM final concentration of forward and reverse PFU create-Hindi III primers, 1µL of

dNTP mix, 1X final concentration of 10X reaction buffer, 1.5µL of Quick Solution Reagent, and 1µL of PFU DNA polymerase. The PCR reaction was performed in MJ Mini Personal Thermal Cycler from Bio-Rad. Thermal cycles consisted of initial denaturation cycle at 95˚C for 2 minutes, followed by 18 cycles with 95˚C denaturation temperature, annealing at gradient of 55˚C, 56.2˚C, 58.4˚C, 61.3˚C, 64.9˚C, and extension at 68˚C for 5 minutes.

Transformation:

Transformation was used to screen for the cells containing the mutation (Hind III cut site), ligation products, as well as for the unmethylated copies of pERFP plasmid (template DNA). Home-made competent cells were thawed on ice for approximately 30minutes. 45 µL aliquot of those cells was transferred to BD Falcon polypropylene round-bottom tube (Catalog #352059) and mixed with 2.0µL (approximately 5µg) of vector DNA containing the mutation (pERFP + Hind III plasmid). The DNA and the cells were incubated on ice for an additional 30minutes. After the incubation the cells were subjected to heat shock for 45seconds at 42˚C in a water bath, and diluted with 0.5mL of NZY medium. The mixture was incubated for approximately 1hour at 37˚C with vigorous shaking at 225rpm. The resulting product was plated on kinamycin (ampicilin in the case of ligation products) agar plates at 37˚C for approximately 16hours. A control reaction was used to eliminate false positive results.

During the screening process 4 colonies were chosen from the transformation plate containing a product of 58.4 ˚C PCR reaction. They were transferred into separate LB falcon tubes containing 8mL of LB medium and 16 µL of 500X kinamycin (no antibiotic in the case of

ligation products), using pipette tips. The cultures were incubated for approximately 12 hours with shaking at 225rpm at 37˚C.

The plasmid was purified from the resulting medium using QIAprep Spin Miniprep Kit (Cat. No. 27104) from Qiagen (procedure closely followed the protocol that accompanies the kit). Concentration of the purified plasmid was measured using a nano-drop instrument.

Restriction Enzyme Digestion:

The product of thermal cycling was treated with 1 µL of Dpn I restriction enzyme in order to digest the methylated, parental template.

Once enough pERFP + Hind III plasmid was prepared, another two 50µL double digestion reactions were set up. One consisted of 5µg of pERFP + Hind III plasmid, 1µL of Hind III restriction enzyme, 1µL of Nhe I restriction enzyme, 5µL of 10XBSA, and 5µL of 10XBuffer 2. Second reaction consisted of 5µg of pMAX(+) plasmid, 1µL of Hind III restriction enzyme, 1µL of Xba I restriction enzyme, 5µL of 10X BSA, and 5µL of 10X Buffer 2.

All of the enzymes and buffer 2 were obtained from New England Bio-labs. The reactions were incubated overnight (approximately 12 hours) in 37˚C water bath.

Dephosphorylation of pMAX(+):

1µL of Calf Intestinal alkaline phosphatase (CIP) was used to dephosphorylate the ends of DNA fragments of the vector (pMax(+) plasmid) after double digestion. The DNA sample and an enzyme were incubated overnight (approximately 12 hours) in a 37˚C water bath. Total reaction volume was 51µL and it contained approximately 5µg of DNA.

Gel Electrophoresis:

Gel electrophoresis was used to separate the DNA fragments of interest after double digestion. First about 200ml of 0.8% agarose gel solution was prepared using electrophoresis grade agarose and a running buffer (40mM Tris-acetate, 1mM EDTA). The resulting solution was heated in a microwave oven until agarose completely dissolved. The solution was poured into the gel-casting unit with a comb in place after it cooled to about 60˚C (on standing). The samples were prepared by adding 6X-loading buffer to bring it to a final concentration of 1X loading buffer (0.04% Bromophenol Blue, 8.3mM EDTA, 6.7% sucrose). When the gel solidified completely the comb was removed and the running buffer was poured over the gel. Finally 20µl of the samples were loaded into each well and the current was applied using Power Pac Basic from Bio-Rad.

After band separation the gel was removed from the casting and soaked in 2.5µg/mL Ethidium bromide solution for approximately 30 minutes. The appropriate bands were cut out using a razor under the Ultra Violet light. QuickClean DNA Gel Extraction Kit form Gen Script Corporation was used in order to purify the DNA fragments from the agarose gel, followed by second purification step using QuickClean 5M PCR Purification Kit from GenScript (Cat. No. L00198). In all purification procedures protocols included in the kits were closely followed.

Ligation:

Rapid DNA Dephos and Ligation Kit from Roche (Cat. No. 04 898 117 001) was used to ligate vector and insert DNA.

Ligation reaction was prepared using approximately 122.5ng of vector DNA, and 73.5ng of insert DNA(mRFP-FKBP12 domain of pERFP plasmid) in a total volume of 7µL, following an addition of 2µL of 5X Buffer included in the kit. The reaction was mixed by centrifugation. Next, 10µL of 2X Buffer (included in the kit) and 1µL of T4 DNA Ligase were added and the sample was mixed well once again.

The sample was incubated at room temperature for approximately one and a half hour. There was a control reaction prepared in which insert DNA was substituted with dH_2O. The control reaction was treated in the same fashion as the reaction containing the insert DNA.

Verification of the identity of the product:

Purified plasmid DNA was digested using Sac I and Not I restriction enzymes. 2µg of DNA was mixed with 5µL of 10XBuffer 1 (10X Buffer 3 in the case of Not I restriction enzyme) from New England Bio-labs, 5µL of 10XBSA, and 1µL of Sac I or Not I restriction enzyme from New England Bio-labs. The reaction mixtures were incubated overnight in a 37˚C water bath.

The identity of products of the above digestion reactions were confirmed using gel electrophoresis. The procedure was the same as described above.

RESULTS:

The results presented in this paper show that we were able to successfully create a plasmid that will be transcribed into cRNA using T7 RNA polymerase, and then injected into Xenopus oocyte, where it will be translated into mRFP-FKBP12 fusion protein.

Introduction of Hind III digestion site:

Since the pMAX(+) plasmid already contains a Hind III cut site and the pERFP plasmid does not, it was necessary to use site directed mutagenesis in order to introduce one into the pERFP plasmid. It was important in the portion of the project in which we attempted to ligate the mRFP-FKBP12 domain of pERFP plasmid with pMAX(+) plasmid.

Site directed mutagenesis consisted of 18 PCR cycles, DpnI restriction enzyme digestion and transformation. 58.4˚C annealing temperature proved to be the best for the introduction of the Hind III digestion site into pERFP plasmid. We were able to successfully transform the resulting product onto the Kinomycin agar plates shown in Figure 2.2a. The lack of colonies on the control plate (Figure 2.2b) indicates that there were no false positive results on the transformation plate (Figure 2.2a). Later digestion of the DNA purified from the transformed colonies has also proven that the Hind III digestion site was successfully introduced into the pERFP plasmid. This can be seen on the agarose gel shown in figure 2.3.

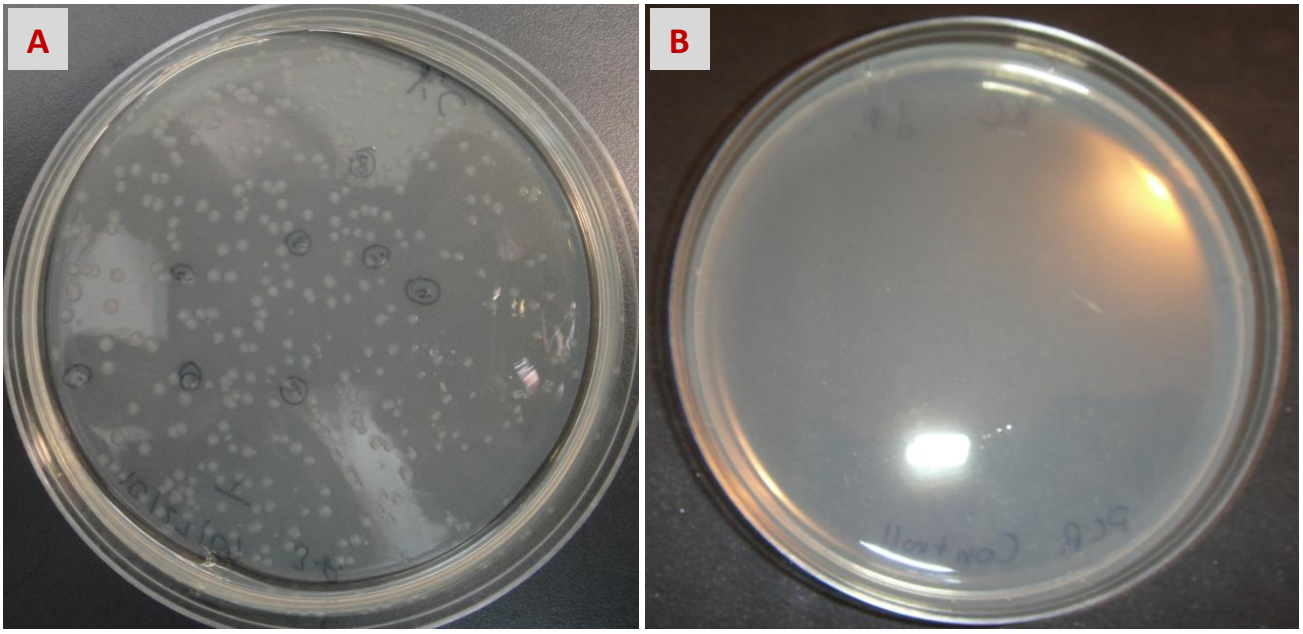

Figure 2.2. Kinamycin agar plates containing transformed 58.4˚C PCR reaction and control reaction. *This figure shows the results of plating transformed pERFP plasmid containing Hind III digestion site along with the control plate. This sample was prepared using 58.4˚C annealing temperature. A) Transformation Plate- multiple colonies are present. Only 4 of those colonies were used further in this project B) Control Plate- no colonies are present.*

Table 2.1. Concentration and purity of pERFP plasmid containing Hind III digestion site.

Colony #	A_{260} 10nm path	A_{280} 10nm path	A_{260}/A_{280}	A_{260}/A_{230}	Concentration [ng/µL]
1	7.620	4.014	1.9	2.37	381.0
2	367.7	3.860	1.9	2.38	367.7
3	417.1	4.386	1.9	2.31	417.1

Purity and concentration parameters measured for the PCR product, using nano-drop instrument, are recorded in table 2.1.

We did not see any colonies on the control plate. This result was expected and proves that PCR reaction was performed correctly. Purity and concentration parameters measured for the PCR product, using nano-drop instrument, are recorded in table 2.1. Concentrations of purified plasmid were quite high and the samples appeared to be pure since both absorbance

rations were higher than 1.8. This data shows that those samples were well suited for further use in the project.

Excision of mRFP-FKBP12 domain and preparation of pMAX(+) plasmid:

In order to isolate the mRFP-FKBP12 domain we used double digestion with Hind III and Nhe I digestion enzyme. We verified the identity of the digestion product using gel electrophoresis (Figure 2.3). The contents of each line in the agarose gel are listed in table 2.2. Both enzymes had compatible buffer requirements what enabled us to perform double digestion in one step instead of performing two single digestions.

Table 2.2. Lane content in the agarose gel prepared for double digesion product of pERFP plasmid.

Line	Contents
1	Traces of 1kb DNA ladder
2	1kb DNA ladder
3	Digested pERFP+Hind III plasmid
4	Digested pERFP+Hind III plasmid
5	Digested pERFP+Hind III plasmid
6	Digested pERFP+Hind III plasmid
7	Digested pERFP+Hind III plasmid
8	Digested pERFP+Hind III plasmid

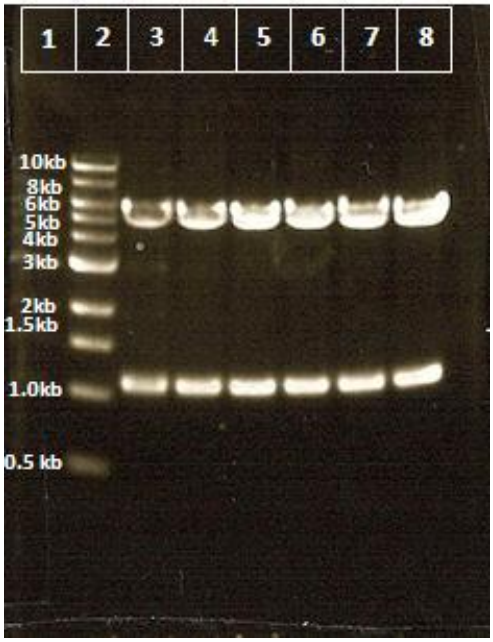

Figure 2.3. Gel electrophoresis for double digested mRFP –FKBP12 domain containing plasmid. *This figure shows the results of double digestion of pERFP+Hind III plasmid. The plasmid underwent digestion by Hind III and Nhe I restriction enzymes producing two bands one around 5kb and another around 1.3kb positions on the agarose gel.*

The bands' separation occurred as expected. Nhe I cuts mRFP-FKBP12 domain containing plasmid at around 600bp and Hind III cuts at around 1670bp position along 6.2kb long plasmid. Therefore, double digestion of the pERFP+Hind III plasmid should produce two fragments, one about 5.0kb long and a second one about 1.3kb long. Those results can be seen in figure 2.3 where the two bands can be clearly seen.

In order to prepare pMAX(+) plasmid for ligation we digested it with Xba I and Hindi III restriction enzymes. Just like Nhe I, Xba I has buffer requirements compatible with Hind III restriction enzyme enabling us to perform one double digestion instead of two single restriction enzyme digestions. Also, Nhe I and Xba I produce compatible ends, which will play an important role in ligation. pMax(+) plasmid contains promoter region that is necessary for a transcription of DNA into cRNA compatible with Xenopus oocyte.

Table 2.3. Lane content in the agarose gel prepared for pMAX(+) double digesion product.

Line	Contents
1	1kb DNA ladder from NEB
2	Blank
3	Digested pMAX(+)
4	Digested pMAX(+)
5	Blank
6	Digested pMAX(+)
7	Digested pMAX(+)
8	Blank

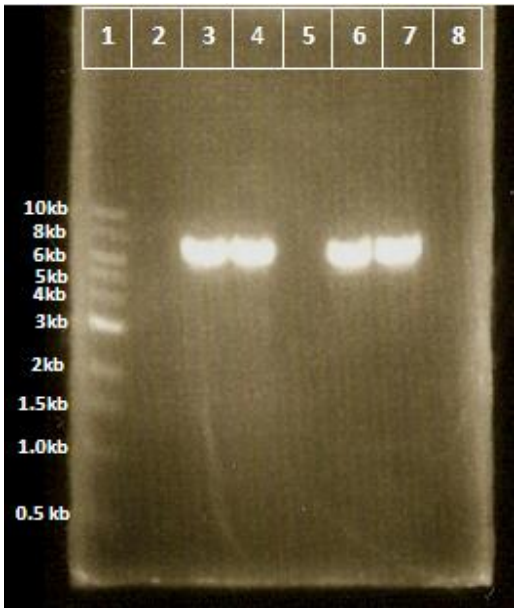

Figure 2.4. Gel electrophoresis for double digested pMAX(+) plasmid. *This figure shows the results of double digestion of the pMAX(+) plasmid. The plasmid underwent digestion by Hind III and Xba I restriction enzymes producing one band around the 5 kb marker on the gel electrophoresis. The second DNA piece produced due to the digestion reaction most likely traveled off of the gel because of its small size.*

Xba I cuts the pMAX(+) plasmid at 887bp position and Hind III cuts at 929bp position. Therefore, there should be two DNA fragments produced from double digestion of the pMAX(+) plasmid, one band around 5.0kb marker and another one around 40bp marker along the plasmid. The second band is too small to be visible on the gel (figure 2.4).

Concentration and purity parameters of the purified vector and insert samples are shown in table 2.4. These values indicate that concentration of the vector DNA was much higher than the concentration of the insert DNA. This was expected since the insert DNA was much shorter than the vector DNA. Sample containing mRFP-FKBP12 domain was purified only once, since second purification could cause a significant DNA loss. Two samples of purified vector DNA were combined in the second purification step in order to increase DNA concentration. Second purification also increased A_{260}/A_{280} ratio, and therefore further purified the samples.

Table 2.4. Purity and concentration of samples containing mRFP-FKBP12 domain and digested pMAX(+) plasmid.

Sample	A_{260} 10nm path	A_{280} 10nm path	A_{260}/A_{280}	A_{260}/A_{230}	Concentration [ng/µL]
mRFP-FKBP only; 1st purification	0.605	0.270	2.24	0.06	30.2
pMAX(+); 1st purification	3.065; 2.437	1.703; 1.306	1.80; 1.87	0.65; 0.33	153.3; 121.8
pMAX(+); 2nd purification	4.058	2.176	1.87	2.06	202.9

The identity of the purified vector and insert samples was once again confirmed using agarose gel electrophoresis. The results presented in figure 2.5 prove that the prepared samples contained digested pMAX(+) plasmid and pERFP+Hind III plasmid. It also proves that the samples were free from contamination with other DNA fragments since only one band in each sample lane was visible.

Table 2.5. Lane contents of the agarose gel prepared for pure, double digested pMAX(+) plasmid and pure mRFP-FKBP12 domain of pERFP plasmid.

Line #	Contents
1	1kb DNA ladder from NEB
2	Blank
3	Pure, digested pMAX(+) plasmid
4	Pure, digested pMAX(+) plasmid
5	Pure, digested pMAX(+) plasmid
6	Pure, digested pMAX(+) plasmid
7	Pure mRFP –FKBP12 domain
8	Pure mRFP –FKBP12 domain

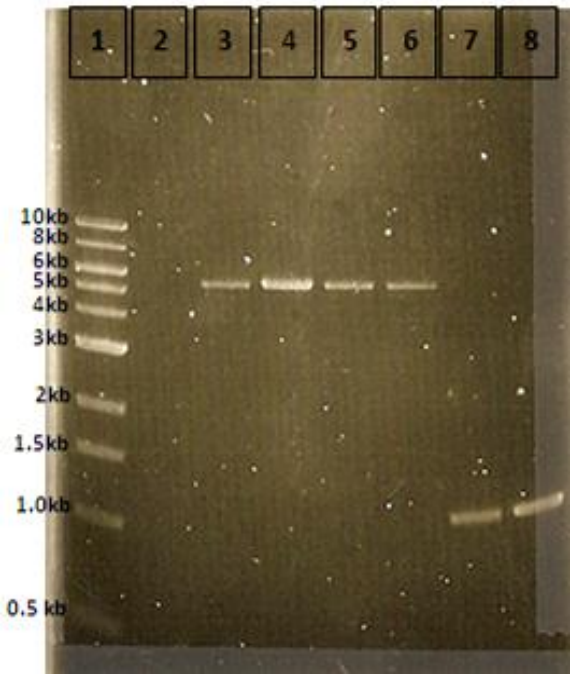

Figure 2.5. Gel electrophoresis for purified pMAX(+) plasmid and mRFP –FKBP12 domain containing plasmids. *This gel was prepared to confirm the identity of the sample extracted and purified from gel electrophoresis. The identity of the samples used in each lane is shown in table 2.5.*

Incorporation of mRFP-FKBP12 domain into pMAX(+) plasmid:

In order to create an mRFP-FKBP12 - pMAX(+) plasmid we performed ligation of mRFP-FKBP12 domain with pMAX(+) plasmid using T4 DNA Ligase. We selected for the ligation product using transformation (Figure 2.6). Ampicillin agar plates were used since pMAX(+) plasmid carries ampicillin resistance genes. After initial 12h incubation at 37˚C only 3 colonies were visible on the ligation plate, two of which are circled in red (Figure 2.6A). The plates were

accidentally left in 37˚C for additional 12h what caused an appearance of other colonies (false positives).

The control plate contained no colonies (Figure 2.6B). This was an expected result since the control ligation reaction contained no vector DNA.

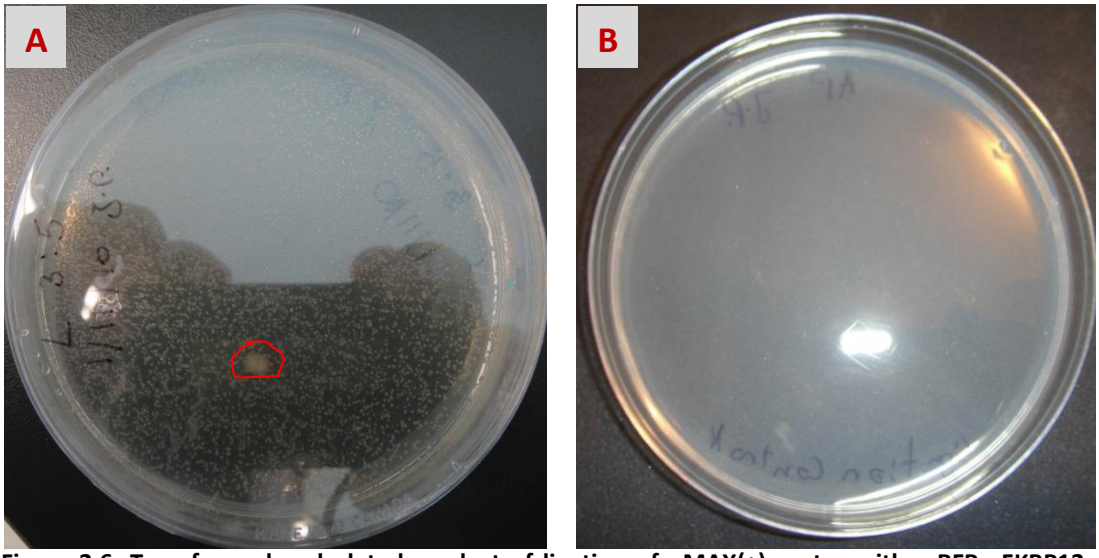

Figure 2.6. Transformed and plated product of ligation of pMAX(+) vector with mRFP –FKBP12 domain. *This figure shows the colonies that grew on a plate after the transformation of the ligation product of vector and inset DNA. The colonies circled in red are the colonies that were visible after the initial 12h incubation at 37˚C. The smaller colonies surrounding the area marked in red formed after the plate was accidentally left for additional 12h at 37˚C, and were not used in this project.*

Confirmation of the identity of the construct:

In order to determine the identity of our construct we used Sac I and Not I digestion of the mRFP-FKBP12 - pMAX(+) plasmid, one reaction at a time.

The results were as expected. Both Sac I and Not I digestion products yielded two bands each on the agarose gel. Both produced one around 5kb. Sac I, also, produced a second band around 1.3kb, and Not I produced a second band around 1kb. These results agree with the

digestion patterns of the two restriction enzymes. Sac I cuts the 6.4kb long mRFP-FKBP12 - pMAX(+) plasmid at 590bp and 1900bp positions producing two DNA fragments, one approximately 1.3kb in length and another one approximately 5.1kb in length. Not I restriction enzyme cuts the construct at around 790bp and 1510bp site along the plasmid also producing two DNA fragments. One fragment is approximately 0.7kb long, and the second one is approximately 5.7kb long.

This exact pattern can be seen in figure 2.7 indicating that the ligation part of the experiment was successful. We are still awaiting the results of automated sequencing which will double check our results.

Table 2.5. Lane contents of the agarose gel prepared for the product of digestion of mRFP-FKBP12-pMAX(+) construct with Not I and Sac I restriction Enzymes.

Line	Contents
1	1kb DNA ladder from NEB
2	Blank
3	Not I digestion product
4	Not I digestion product
5	Blank
6	Sac I digestion product
7	Sac I digestion product
8	Blank

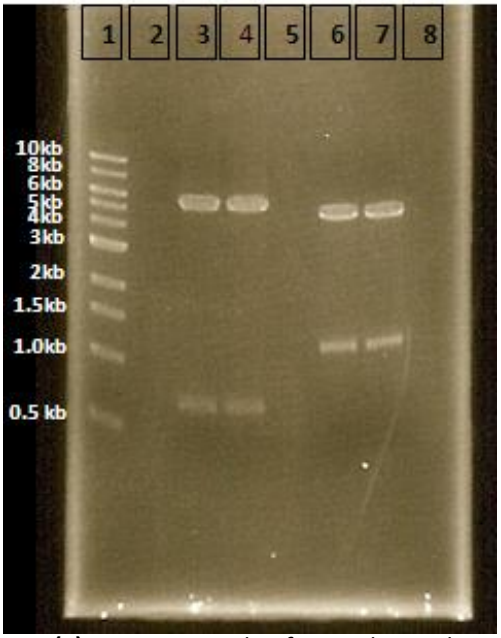

Figure 2.7. Gel electrophoresis for digested mRFP –FKBP12 –pMAX(+) construct. *This figure shows the agarose gel electrophoresis results for the mRFP –FKBP12 -pMAX(+) construct digested with Not I (lanes 3 and 4) and Sac I (lanes 7 and 8). This gel was used to confirm the identity of the ligation products. Identities of the samples loaded in each lane are listed in table 2.5.*

DISCUSSION:

The data presented above indicates that we have succeeded in creating a DNA plasmid required for expression of mRFP-FKBP12 fusion protein in Xenopus oocytes. At each stage we were able to obtain DNA of good quality. After each purification step the DNA concentration of the samples was relatively high. The quality of the samples was measured using A_{260}/A_{280} ratios, which are indicative of protein contamination. In each case this ratio was higher or at least equal to 1.8. This means that these samples had good enough quality to be used in the further stages of the experiment and the protein concentration in the samples was small enough so that it would not inhibit any of the enzymatic reactions that had to be carried out after purification.

The identity of the DNA samples was successfully confirmed using gel electrophoresis before and after the ligation stage of this project. The pERFP plasmid was successfully digested at two sites, producing DNA fragment of interest (fragment containing mRFP- FKBP12 domain). This fragment is about 1.3kb in size and has ends compatible to the DNA fragment produced by double digestion of the pMAX(+) plasmid.

Ligation results were confirmed in the same fashion. First, the use of control plate ensured that there were no false positive results, since there were no colonies visible on that plate. Then the double digestion resulted in the expected bands on the agarose gel. According to the genetic map of the mRFP –FKBP12-pMAX(+) plasmid it has two Not I digestion sites, at 590bp and 1900bp positions along the nucleotide chain. Since this plasmid is expected to be about 6.4 kb long, Not I digestion should yield two DNA fragments, one about 1.3kb and the

other about 5.1kb long. Similarly, there are two Sac I digestion sites at the 790bp and 1510bp positions of the nucleotide chain. Digestion with this restriction enzyme was expected to produce fragments about 1kb and 5kb long. Since the bands on the agarose gel containing the digested samples revealed the pattern very close to the one just described, we can be quite sure that the product of the ligation reaction is indeed the mRFP –FKBP12-pMAX(+) plasmid. To double check these results, the samples were also sent for automated sequencing.

Once the data is fully confirmed, so that there is no doubt as to the sequence of designed plasmid, we will proceed to transcription of this DNA into cRNA using T7 RNA polymerase. This nucleotide chain will then be used in the studies of the activity of potassium ion channels using Xenopus oocytes as a model organism. The construct prepared in this project will be used as a negative control since it lacks the 5-phosphatase domain. It will be able to heterodimerize with FRB-CFP construct but will not be able to dephosphorylate PIP_2 leaving its concentration unchanged.

Injection of cRNA into Xenopus oocytes are expected to result in 100% of the injected genetic material being translated into protein products which will enable us to easily manipulate the concentration of the protein constructs in the oocyte [12]. The efficiency of the translation will be visible due to the mRFP portion of the construct.

CONCLUSION:

The only conclusion that can be made at this stage is that the construct was successfully created. This is confirmed by multiple pieces of data, most importantly gel electrophoresis of two cut digestions by Not I and Sac I restriction enzymes presented in figure2.7. Those results will also be confirmed using automated sequencing analysis performed by a second party.

REFERENCES:

1. Rouleau G, Gaspar C (2008) *Academic Press,* USA Vol.63.
2. Towbin JA, Vatta M (2001) *Am J Med* 110:385-398.
3. Jentsch TJ (2000) *Nature* 1:21-30.
4. Toker A, and Cantley CL (1997) *Nature* 387:673-676.
5. Loussouarn G, Park KH, Bellocq C, Baro I, Charpentier F, Escande D (2003) *EMBO J* 22:5412-5421.
6. Hilgemann WD, Feng S, Nasuhoglu C (2001) *Sci STKE* 2001:re19.
7. Varnai P, Thyagarajan B, Rohacs T, Balla T (2006) *J Cell Biol* 175:377-382.
8. McLaughlin S (2006) *Science* 314:1402-1403.
9. Suh BC, Hille B (2005) *Curr Opin Neurobiol* 15:370-378.
10. Suh CB, Inoue T, Meyer T, Hille B (2006) *Science* 314:1454-1457.
11. Varani P, Balla T (2007) *Eur J Physiol* 445:69-82.
12. Liu XJ (2006) *Humana Press*, Totowa NJ.